ZEISS Semiconductor Manufacturing Technology

Enabler for smaller, more powerful and energy-efficient microchips

Eric Pellegrin (SMT-DTMC)
Carl Zeiss SMT GmbH

Agenda

SMT covers variety of processes in production of microchips

With three strategic business units & as a segment of the ZEISS Group

01 | SMO

Semiconductor Manufacturing Optics

- Lithography optics
- Mirror blocks and wafer chucks
- Optical systems, metrology devices and components for wafer inspection and lithography lasers
- Synchrotron optics
- Collectors

02 | SMS

Semiconductor Mask Solutions

- Mask metrology
- Mask tuning
- Mask repair
- Mask qualification
- Automation applications

03 | PCS

Process Control Solutions

- Multibeam electron microscope (Multi SEM/eBeam)
- 3D Tomography
- NanoFab CE

Optical Lithography

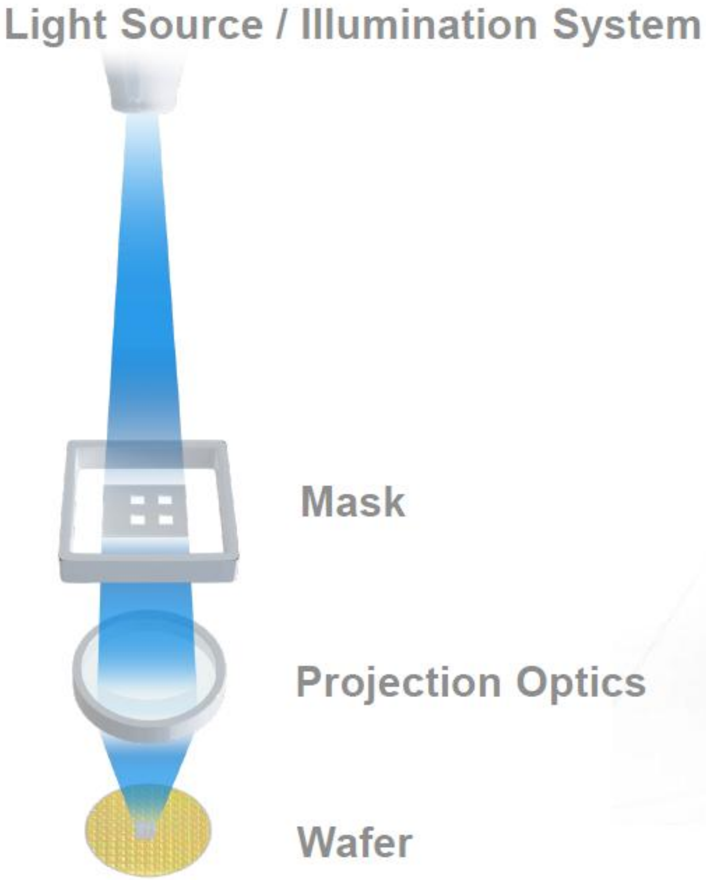

ASML stratetic partnership ZEISS

Around **80 percent** of the world's microchips are manufactured using **ASML lithography** systems with **ZEISS optics**.

Optical innovations have enabled the continuation of Moore's Law

Projection Lithography

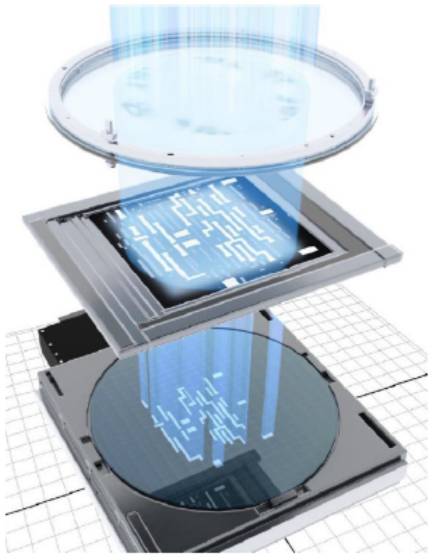

$$\Delta x = \kappa \frac{\lambda}{NA}$$

Evolution

Asphere technology
High NA, compact designs

Evolution

Catadioptric Designs
Immersion hyper-NA>>1

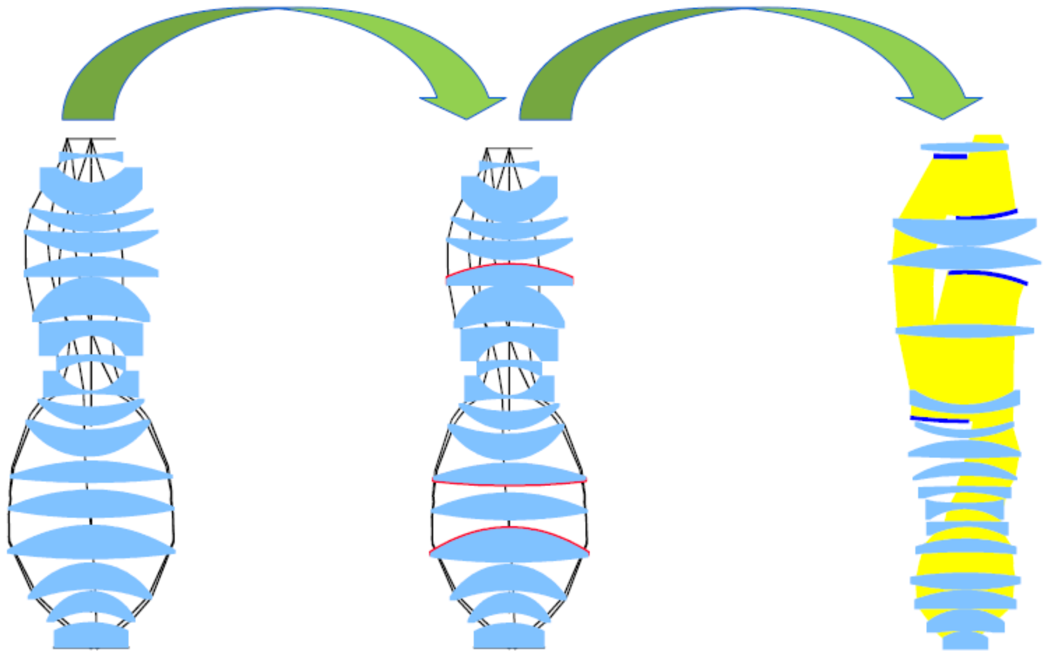

KrF, 248nm
NA 0.80
1995

ArF dry, 193nm
NA 0.93
2000

ArF Immers., 193nm
NA 1.35
2007

Quantum Leap

Mirror only EUV optics
in Vacuum

- 10x less surfaces
- 10x better correction needed
- Environmental control needed
- No rot. Symmetry / dynamics

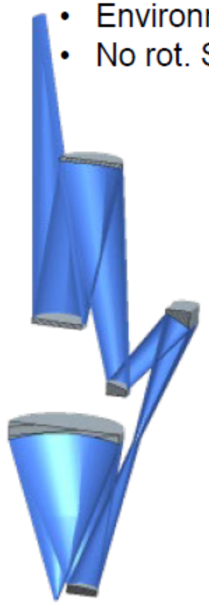

EUV, 13.5nm
NA 0.33 – …
2020 – 20XX

Modern lithography machines contain various subsystems & components developed and manufactured by SMT

Deep Ultraviolet (DUV)

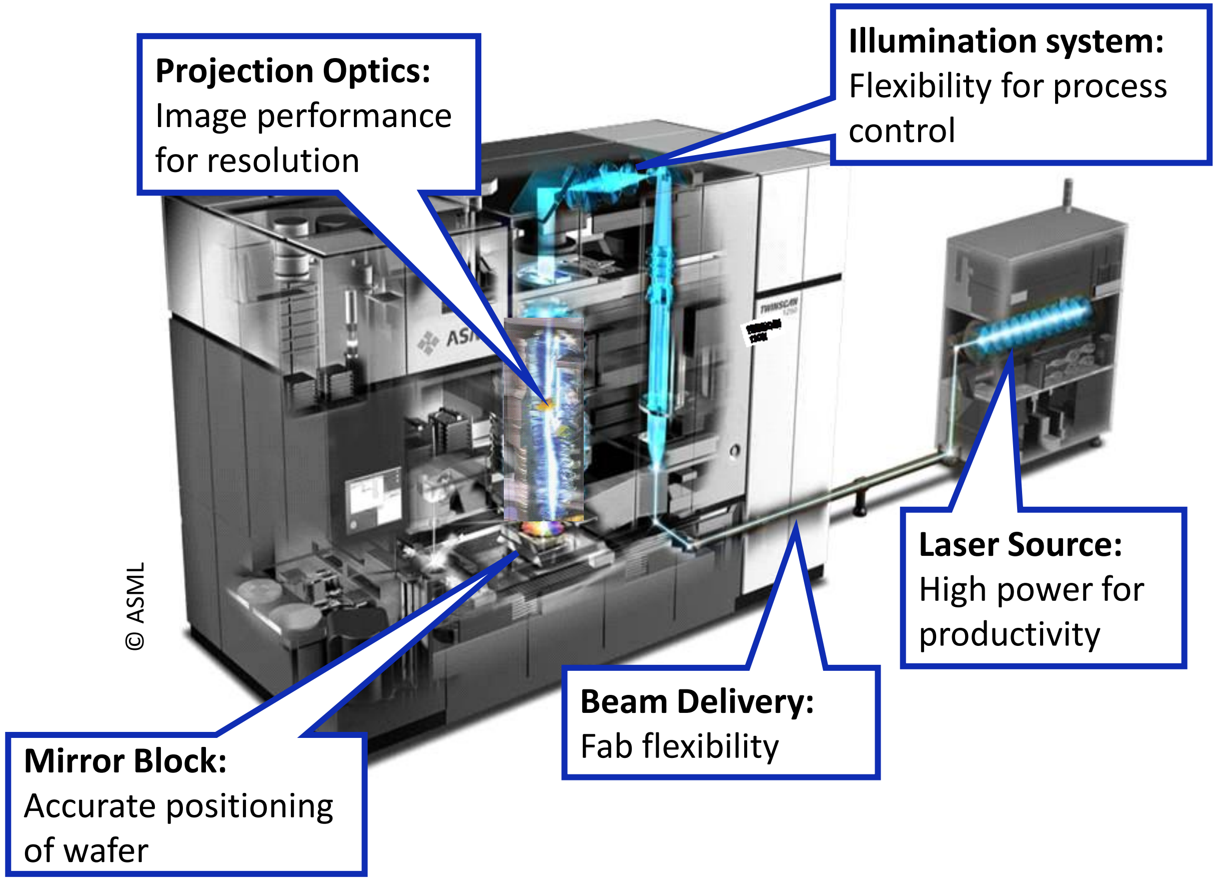

Extreme Ultraviolet (EUV)

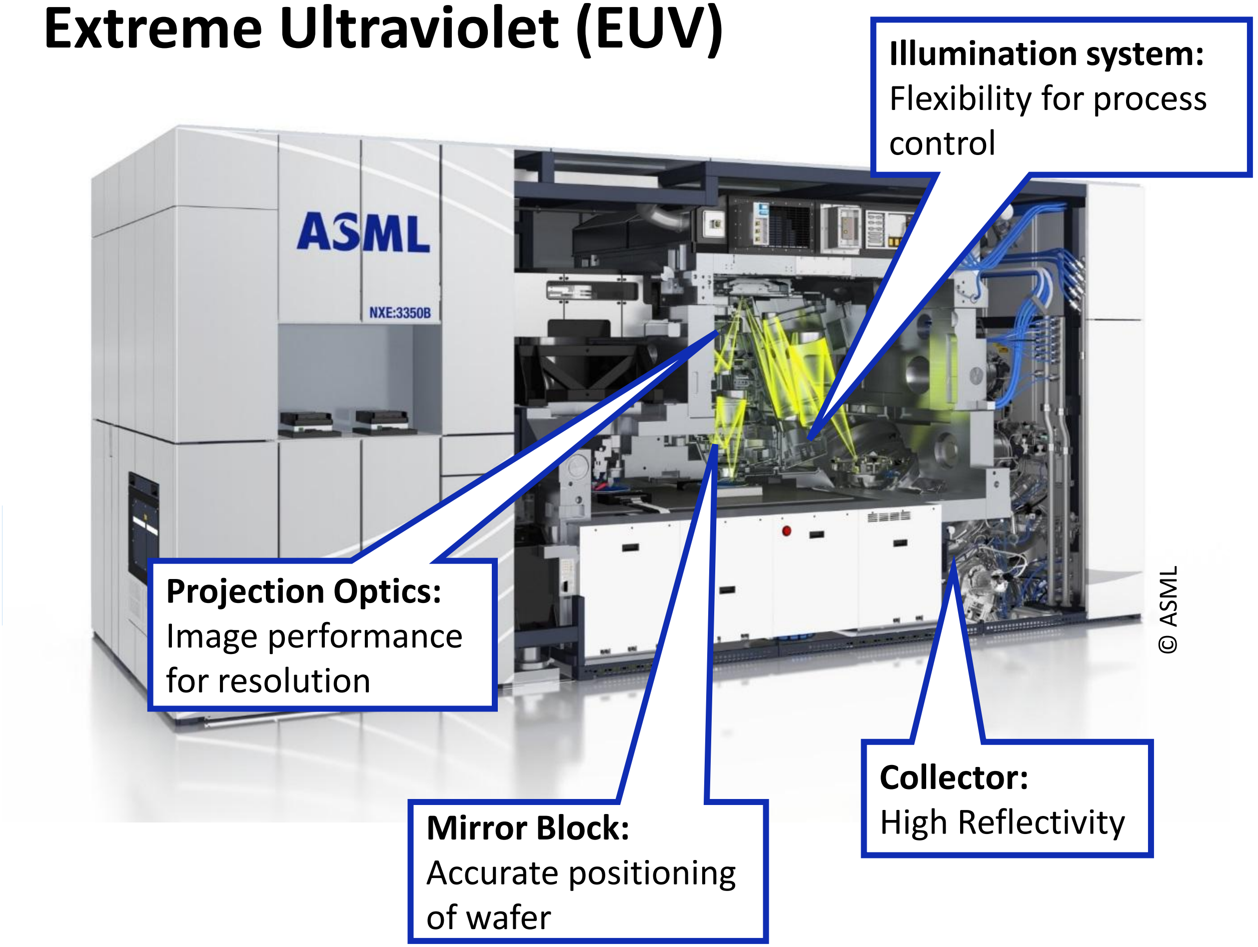

The Optical Train of an EUV Lithography System

Illumination
Fly's Eye Integrator

Switchable facets
for use case specific
light distribution

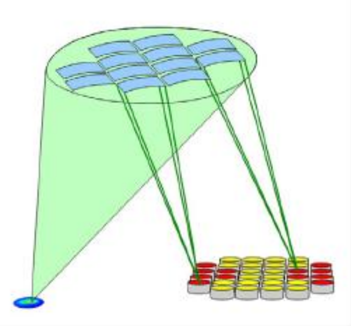

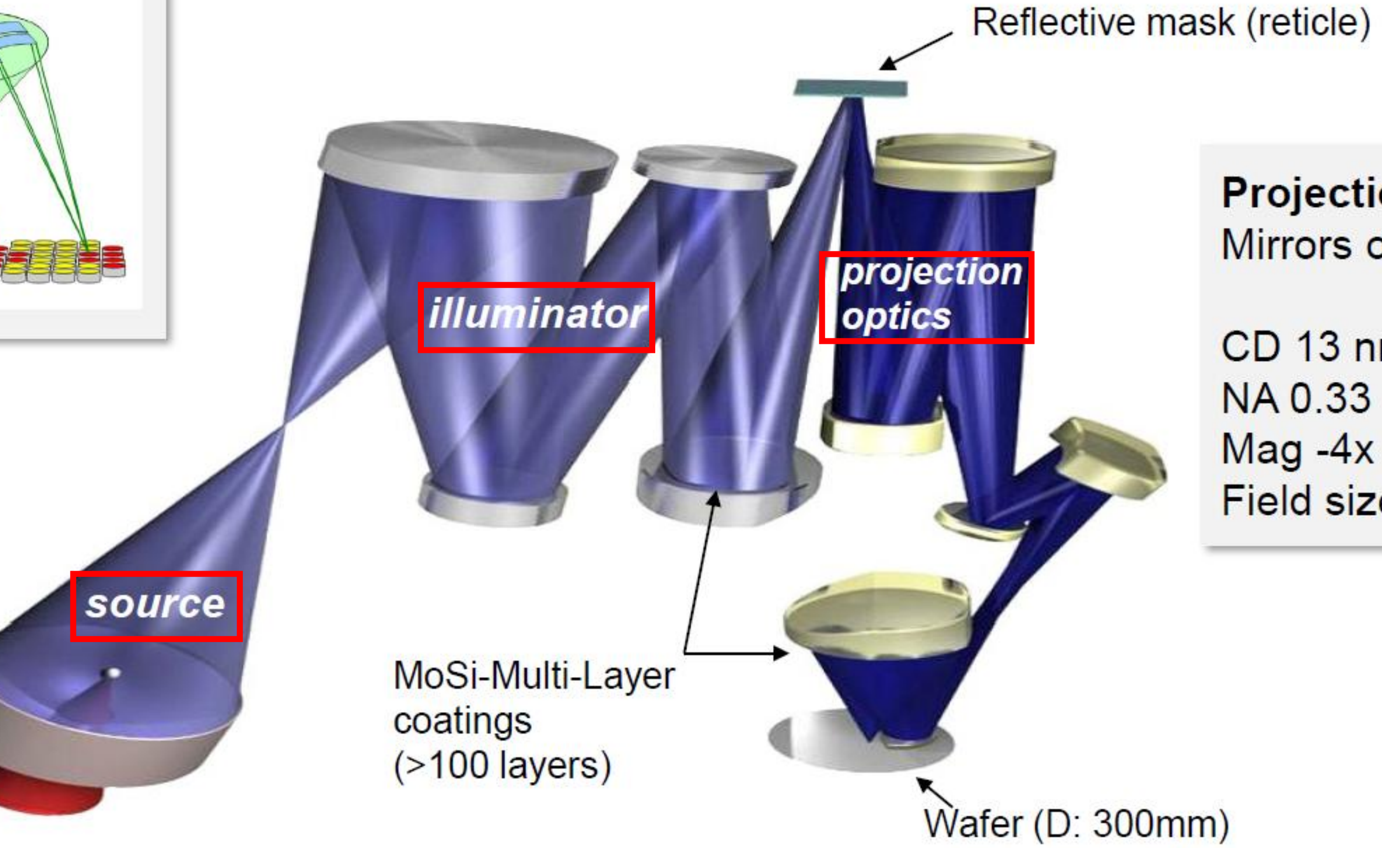

Projection Optics
Mirrors only (aspheric)

CD 13 nm
NA 0.33
Mag -4x
Field size 26 x 33 mm²

Plasma Light Source
40 kW CO_2 laser
hitting a tin droplet
at 50kHz rep rate,
emitting EUV at λ = 13.5 nm

Agenda

Opportunities for EUV Optics & Materials with Synchrotron Analytics
Past, present, and possible future

EUV optics and multilayers

- Optics lifetime (OLT) aspects and studies.

→EUV ML degradation mechanisms.

→ Mitigitation strategies

- Contamination aspects (hydrogen-induced outgasing etc.)
- GISAXS on EUV MLs
- Hydrogen plasma-surface interactions.

→ NAP-XPS@Plasma

EUV engineering materials

- Hydrogen plasma-induced material degradation (chemistry, crystal structure, morphology)
- Corrosion on fluid cooled systems.

EUV-driven hydrogen plasma studies

- *At wavelength (13.5 nm)* in situ studies of hydrogen plasma/surface interaction.
- *At wavelength (13.5 nm)* investigations of secondary (electron) processes & photolectron yield studies.

Optical & mechanical metrology (at ALS, BESSY, ALBA)

- Micro-stepper studies as EUVL Proof of Principle.
- EUV ML mirror and coating metrology.
- Optical metrology on mirror surfaces (EUV & beamline optics)
- Mechanical metrology on UHV systems for EUV applications.

Agenda

Example 1: PEEM Studies on EUV ML systems
Contaminations on EUV Witness Samples (WiSas) from Illuminator
"What are the white dots made of?"

ALBA CIRCE Beamline 24

PEEM branch

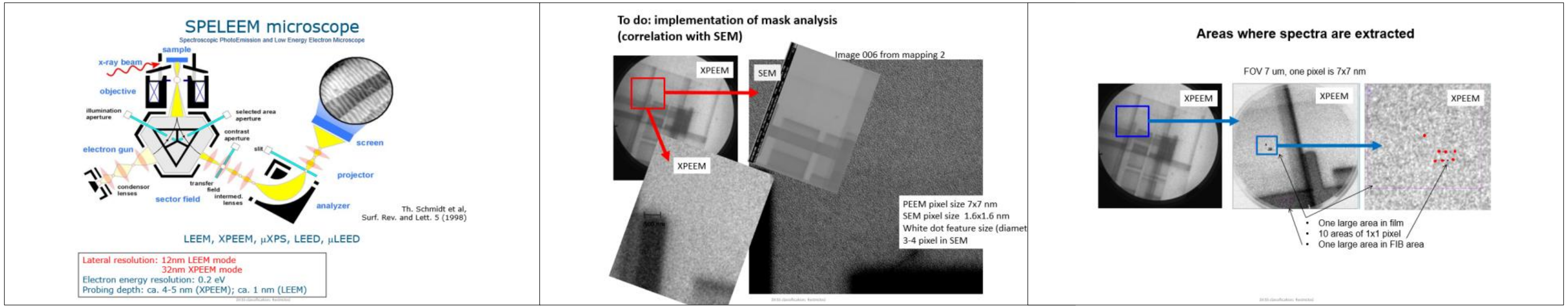

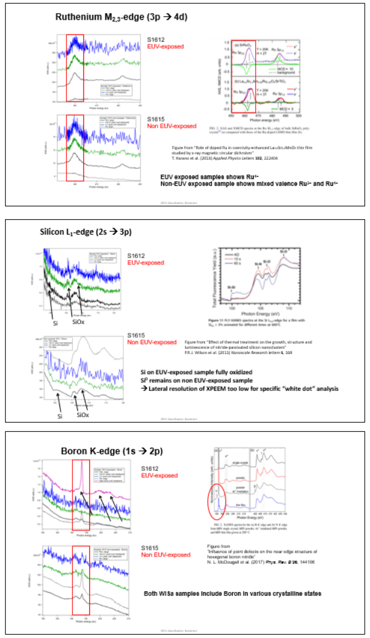

Context:

- EUV ML Witness Samples (WiSas) from Illuminator – EUV-exposed and non EUV-exposed.
- EUV-exposed WiSas do show contaminations as „white dots" on a nanometric scale.

→ Root cause analysis on „white dot" contamination required

Targeted analysis:

- Combination of:
  - PEEM imaging - chemical mapping with medium lateral resolution
  - SEM imaging – high lateral resolution with low chemical lateral resolution.

….using sample reference markers and numerical image analysis. → **Future improved AI imaging analysis?**

Agenda

Example 2: NEXAFS Studies on MgF_2-Protected Al Mirrors
Example from VUV wafer inspection optics, but still holds as an example for EUV.

ALBA CLAESS Beamline 22

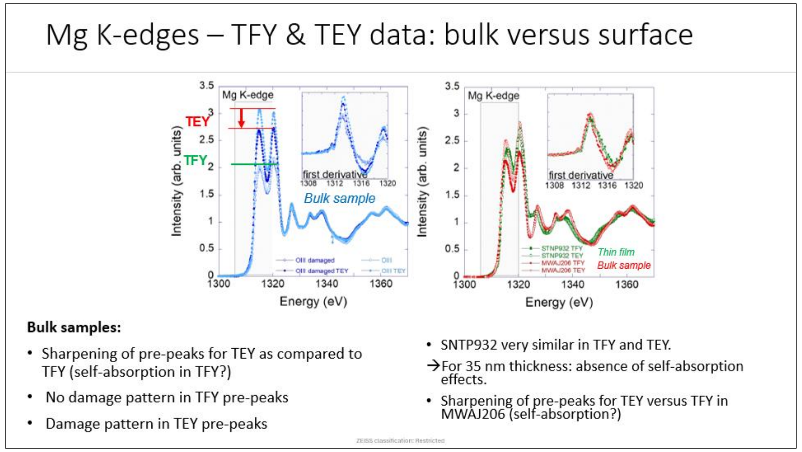

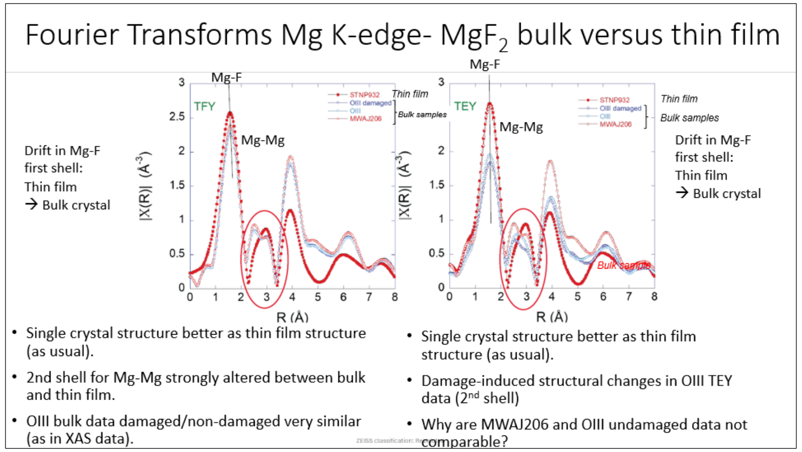

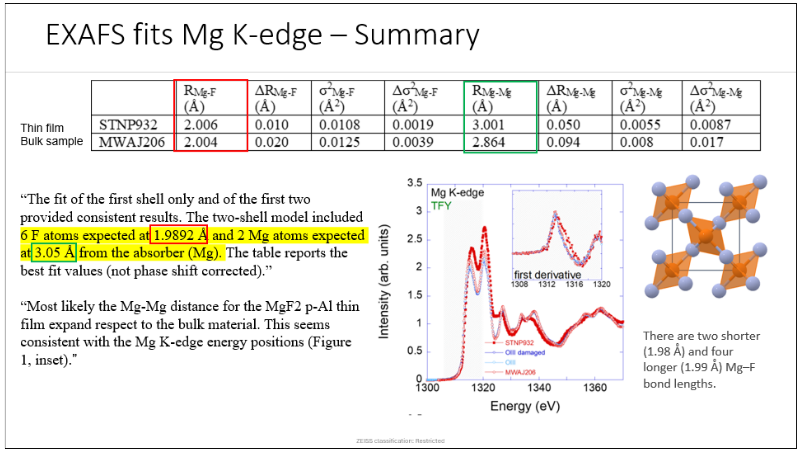

Context: MgF_2-protected Al mirrors for VUV applications

- Al is the ideal reflective coating for the VUV range
- Starting point: use MgF2 as a protective coating

→ Seems pretty standard, but rather difficult in terms of optics lifetime aspects under intense VUV irradiation.

Targeted analysis:

- Structural quality of bulk vs. thin film MgF_2
- Structural and chemical changes of MgF2 thin films on the atomic level (e.g., Fluorine dislocation and vacancies) under intense VUV irradiation

→ Impact on optics lifetime and thin film processing

Agenda

One outlook: NAP-XPS@Plasma
A first approach → Proof of Principle successfull

Possible target:

ALBA 3Sbar Beamline 15

Objective:

- In-situ and „live“ study of surface-plasma interactions during EUV-induced plasma exposure
- „Live“ XPS study of surface chemistry dynamics as a function of exposure time & plasma parameter variation

Issues:

- Protect XPS analyzer electron optics from interaction with plasma (basically electric shorts)
- Discriminate x-ray photoelectrons from electrons in plasma

  (→ highly different kinetics)

Approach:

- Standard off-the-shelf differential pumping approach for XPS analyzer and x-ray source (1 to 20 Pa is not a problem)
- Further modifications / adaptations on analyzer entrance lens (if any) in cooperation with XPS analyzer manufacturer

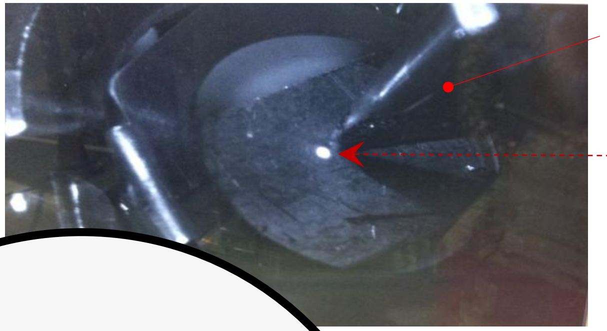

Zero order beam at sample.

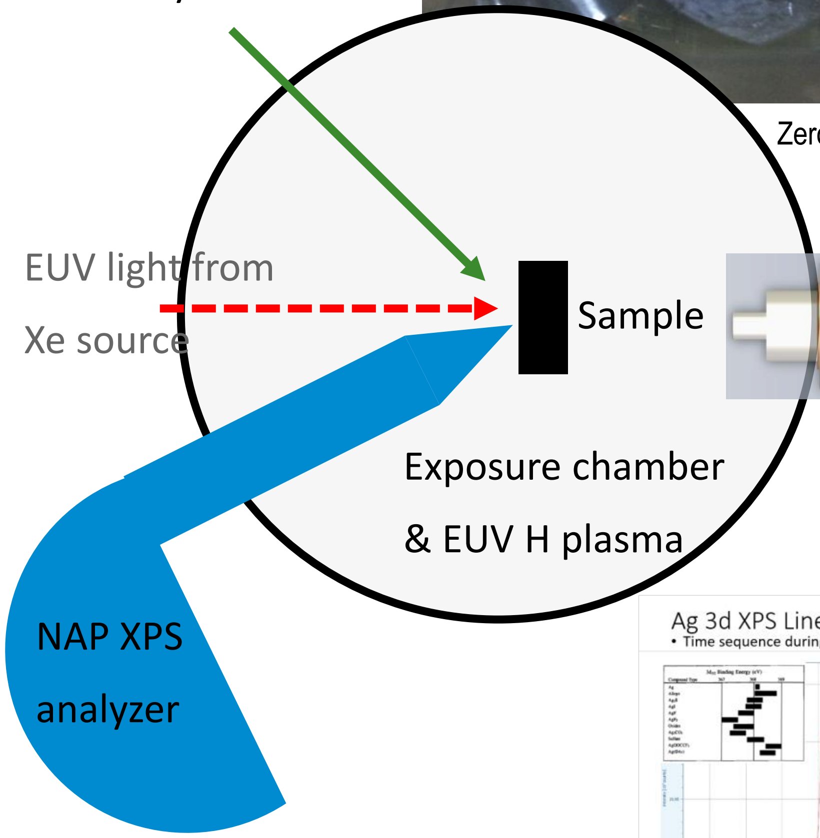

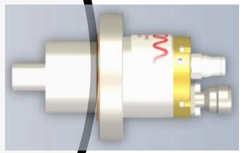

ECR plasma source

(2.5 GHz,

100 W MW power)

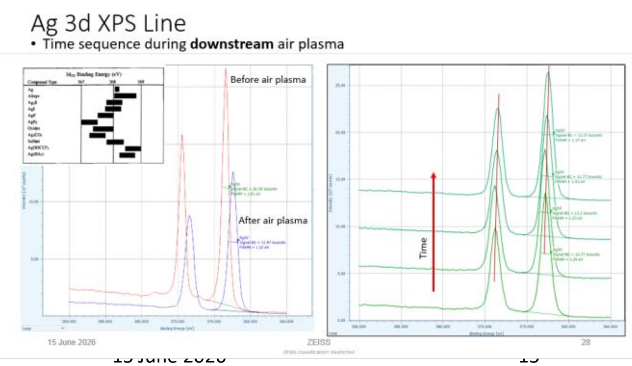

Objective:

Combination of in situ chemical & structural analytics under hydrogen plasma conditions.

Agenda

Opportunities for EUV Optics & Materials with Synchrotron Analytics

Past, present, and possible future

EUV optics and multilayers

- Optics lifetime (OLT) aspects and studies.

→EUV ML degradation mechanisms.
→ Mitigitation strategies

- Contamination aspects (hydrogen-induced outgasing etc.)
- GISAXS on EUV MLs
- Hydrogen plasma-surface interactions.

→ NAP-XPS@Plasma

EUV engineering materials

- Hydrogen plasma-induced material degradation (chemistry, crystal structure, morphology)
- Corrosion on fluid cooled systems.

EUV-driven hydrogen plasma studies

- *At wavelength (13.5 nm)* in situ studies of hydrogen plasma/surface interaction.
- *At wavelength (13.5 nm)* investigations of secondary (electron) processes & photolectron yield studies.

Optical & mechanical metrology (at ALS, BESSY, ALBA)

- Micro-stepper studies as EUVL Proof of Principle.
- EUV ML mirror and coating metrology.
- Optical metrology on mirror surfaces (EUV & beamline optics)
- Mechanical metrology on UHV systems for EUV applications.

ZEISS

Seeing beyond

SPELEEM microscope

Spectroscopic PhotoEmission and Low Energy Electron Microscope

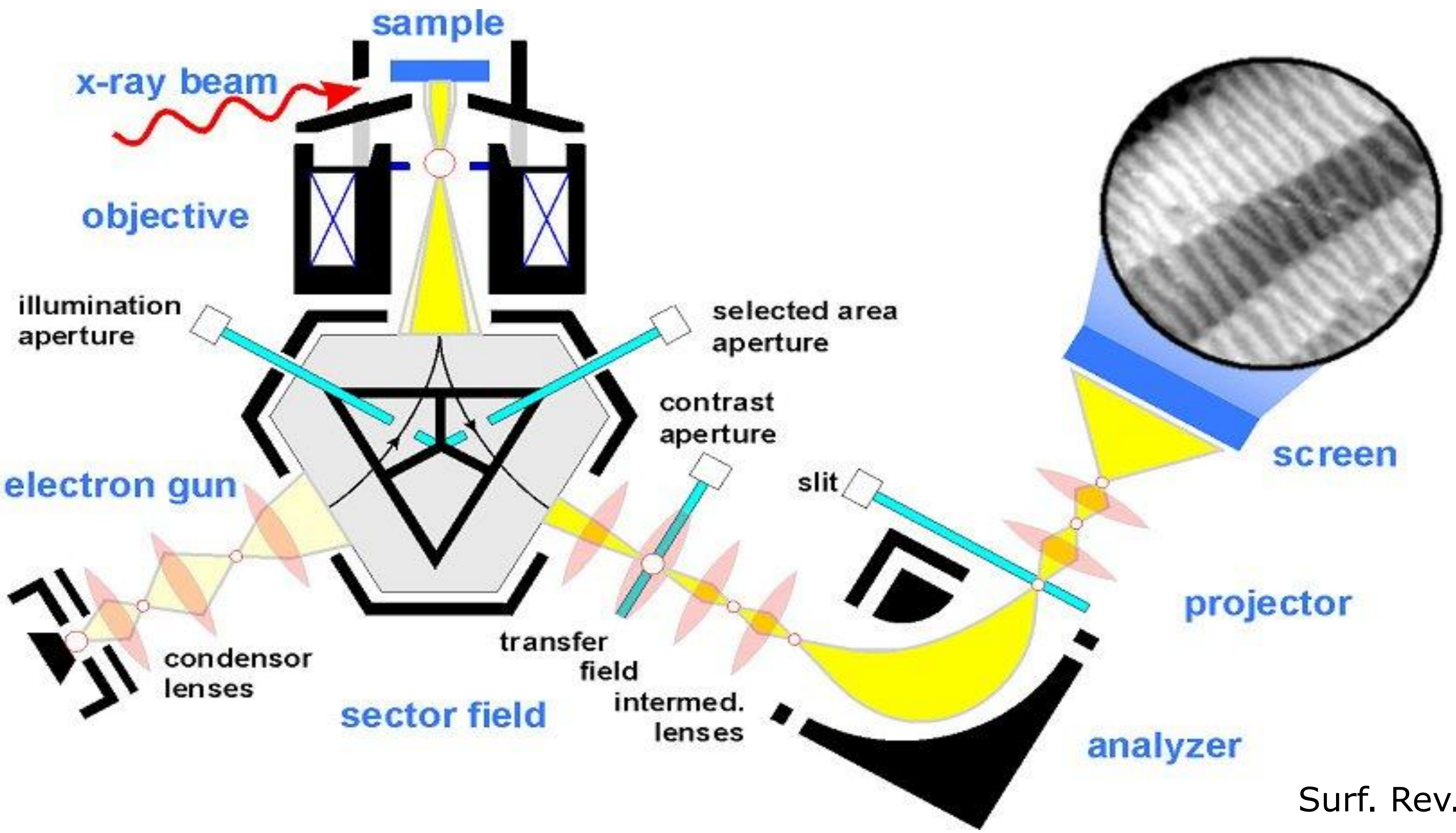

Th. Schmidt et al,
Surf. Rev. and Lett. 5 (1998)

LEEM, XPEEM, μXPS, LEED, μLEED

Lateral resolution: 12nm LEEM mode
32nm XPEEM mode
Electron energy resolution: 0.2 eV
Probing depth: ca. 4-5 nm (XPEEM); ca. 1 nm (LEEM)

To do: implementation of mask analysis (correlation with SEM)

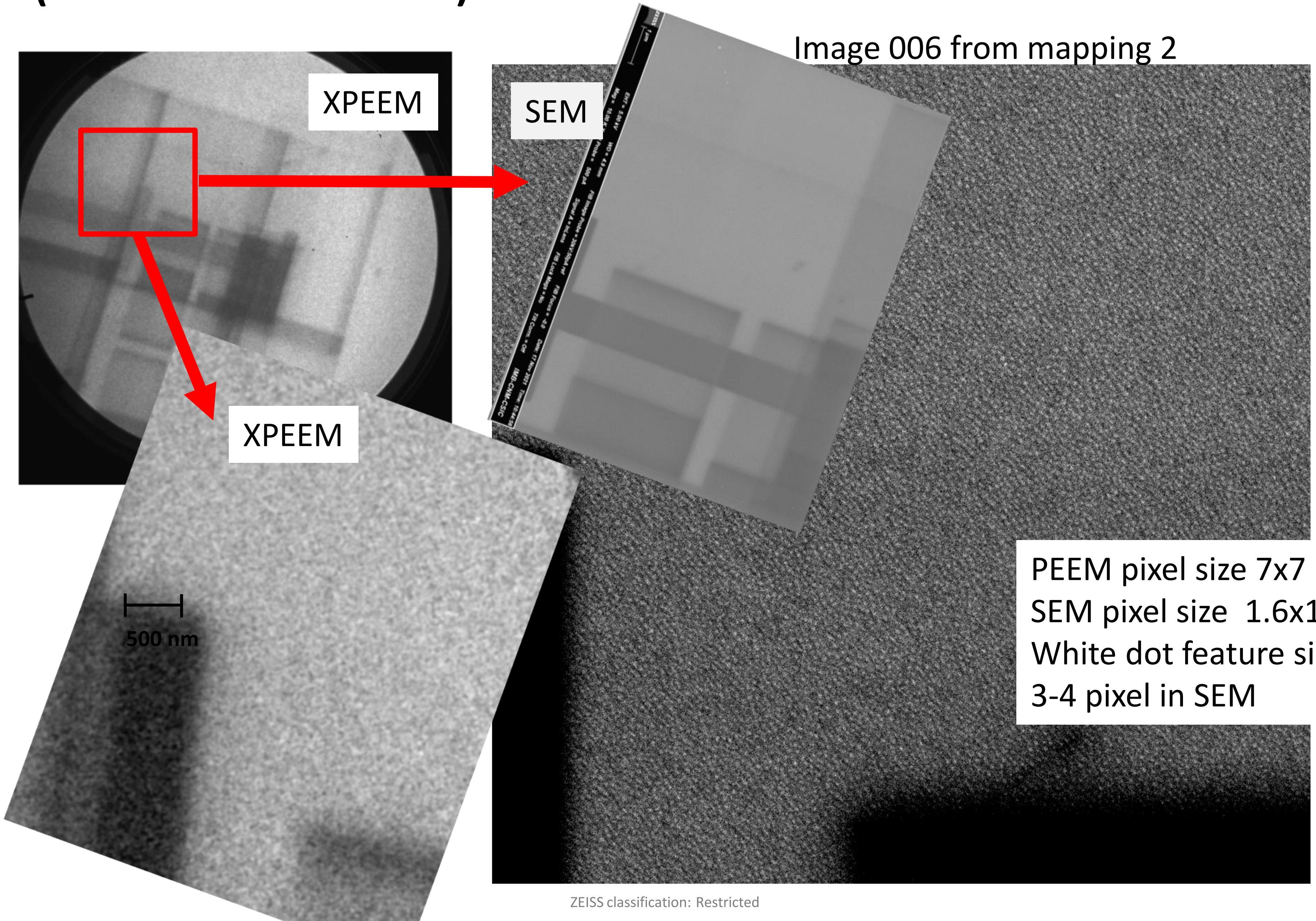

PEEM pixel size 7x7 nm
SEM pixel size 1.6x1.6 nm
White dot feature size (diameter):
3-4 pixel in SEM

Areas where spectra are extracted

FOV 7 um, one pixel is 7x7 nm

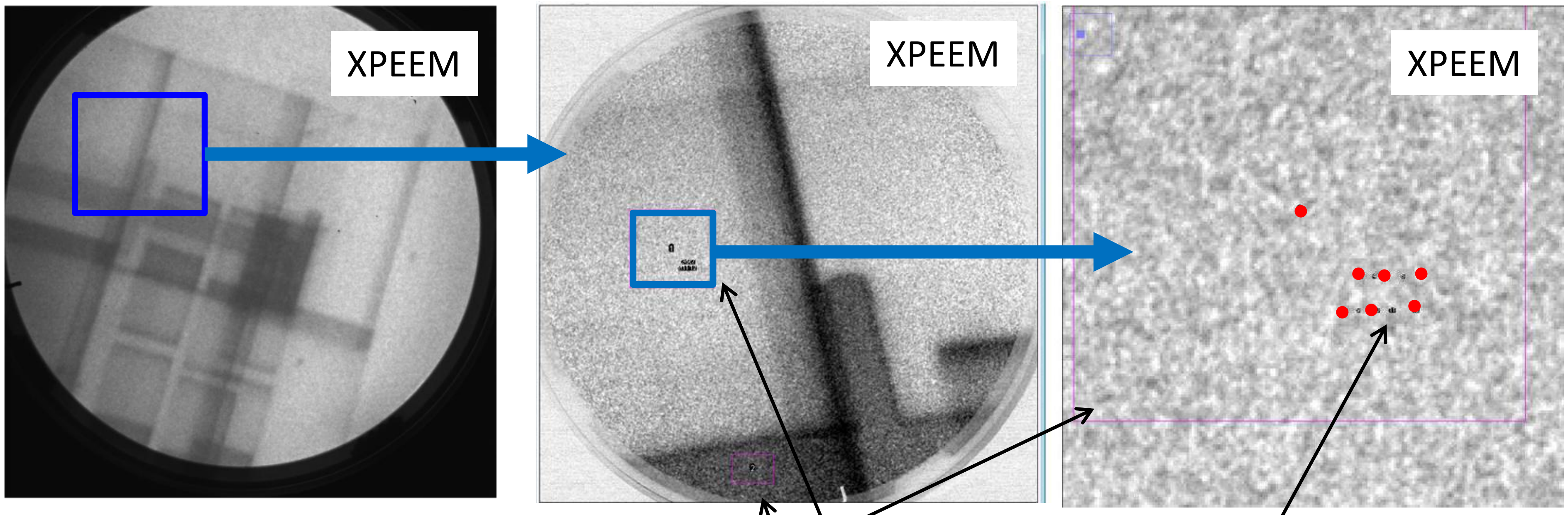

- One large area in film
- 10 areas of 1x1 pixel
- One large area in FIB area

Ruthenium $M_{2,3}$-edge (3p → 4d)

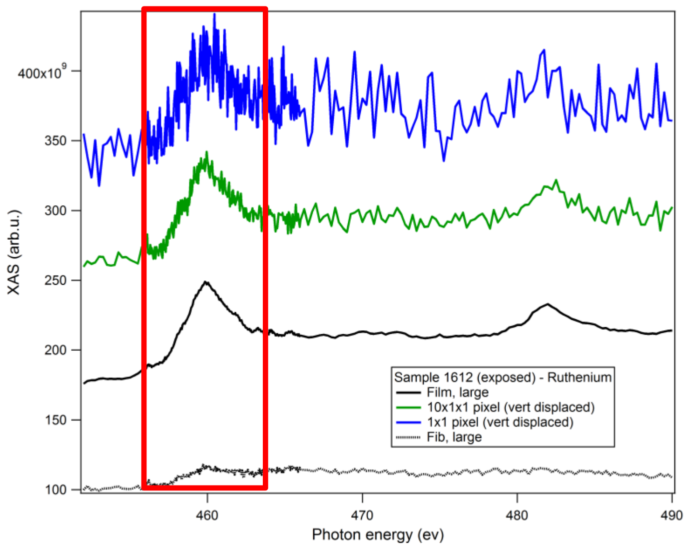

S1612
EUV-exposed

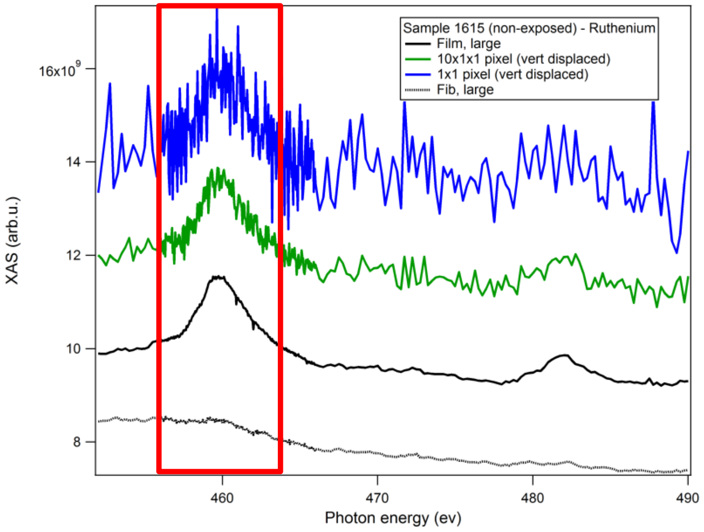

S1615
Non EUV-exposed

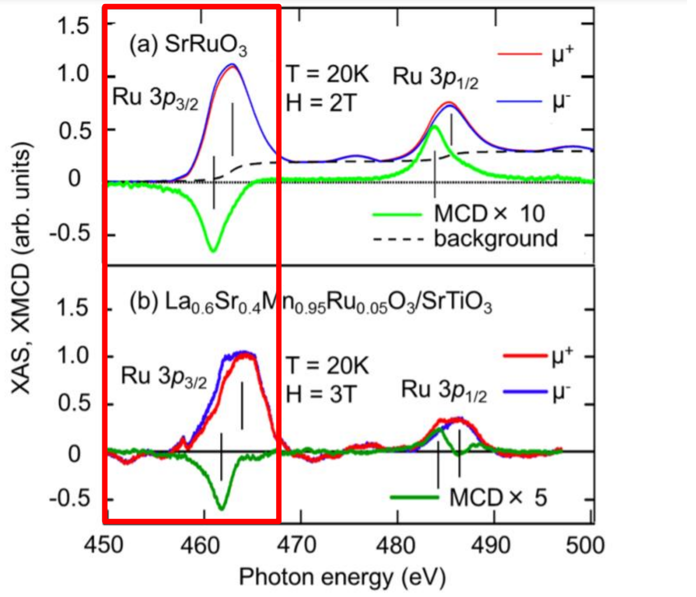

FIG. 2. XAS and XMCD spectra at the Ru $M_{2,3}$ edge of bulk $SrRuO_3$ polycrystal[10] (a) compared with those of the Ru-doped LSMO thin film (b).

Figure from "Role of doped Ru in coercivity-enhanced $La_{0.6}Sr_{0.4}MnO_3$ thin film studied by x-ray magnetic circular dichroism"
T. Harano et al. (2013) *Applied Physics Letters* **102**, 222404

EUV exposed samples shows Ru^{4+}
Non-EUV exposed sample shows mixed valence Ru^{3+} and Ru^{4+}

Silicon L_1-edge (2s → 3p)

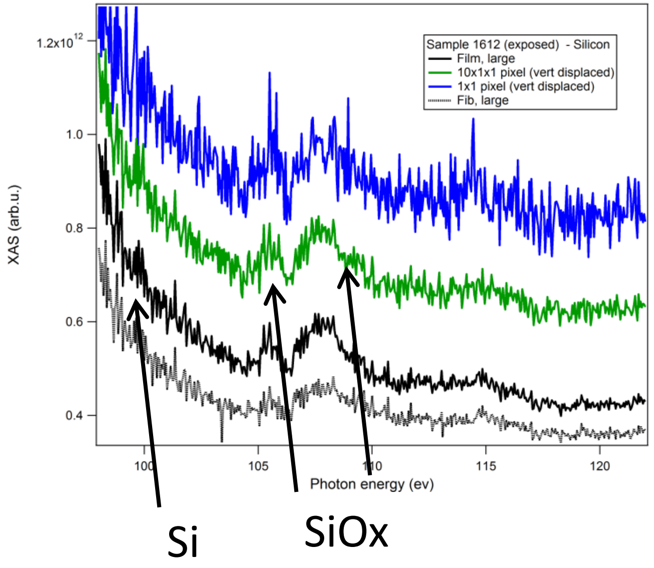

S1612
EUV-exposed

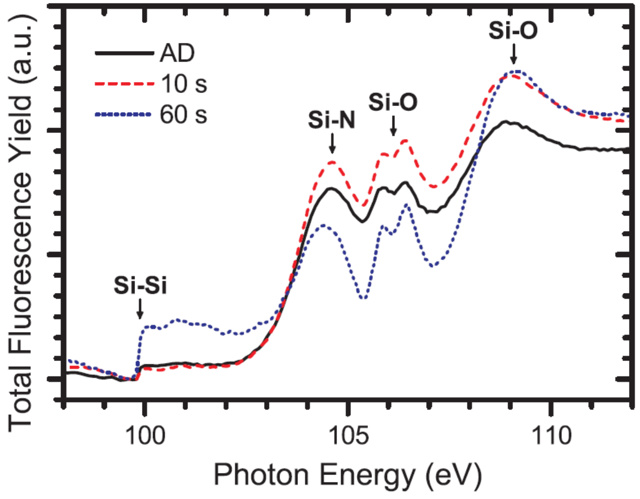

Figure 11 FLY-XANES spectra at the Si $L_{3,2}$-edge for a film with Si_{ex} = 3% annealed for different times at 600°C.

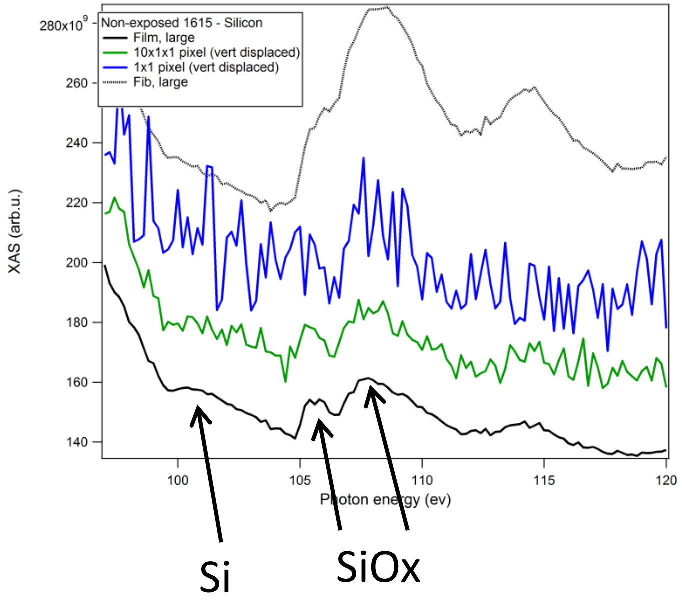

S1615
Non EUV-exposed

Figure from “Effect of thermal treatment on the growth, structure and luminescence of nitride-passivated silicon nanoclusters”
P.R.J. Wilson et al. (2011) *Nanoscale Research letters* **6**, 168

Si on EUV-exposed sample fully oxidized
Si^0 remains on non EUV-exposed sample
→ Lateral resolution of XPEEM too low for specific “white dot” analysis

Boron K-edge (1s → 2p)

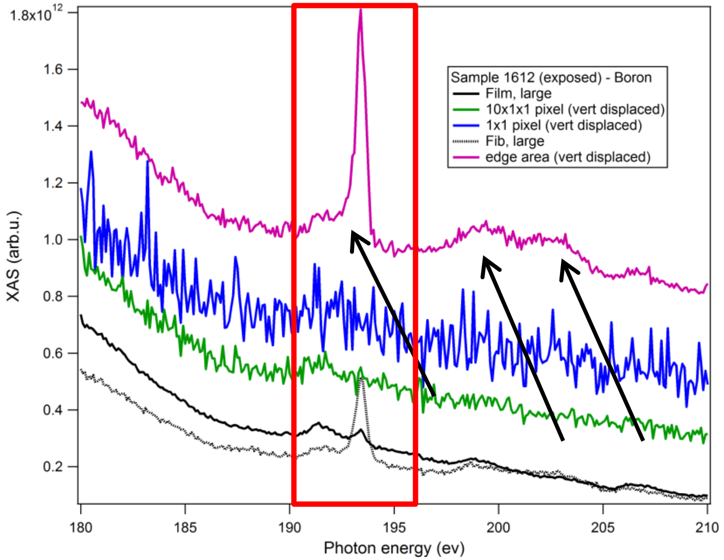

S1612

EUV-exposed

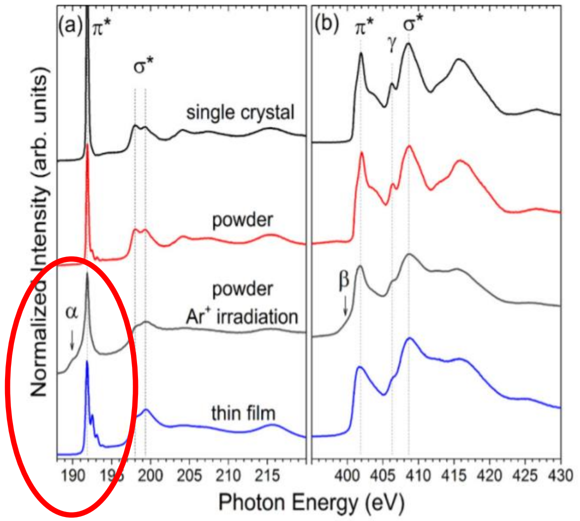

FIG. 2. XANES spectra for the (a) B K edge and (b) N K edge from hBN single crystal, hBN powder, Ar^{+} irradiated hBN powder, and hBN thin film grown at 200 °C.

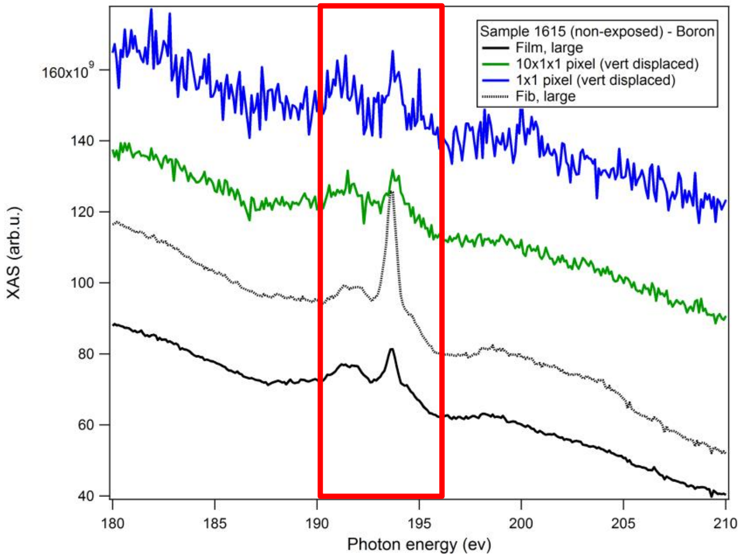

S1615

Non EUV-exposed

Figure from
"Influence of point defects on the near edge structure of hexagonal boron nitride"
N. L. McDougall et al. (2017) *Phys. Rev. B* **96**, 144106

Both WiSa samples include Boron in various crystalline states

Mg K-edges – TFY & TEY data: bulk versus surface

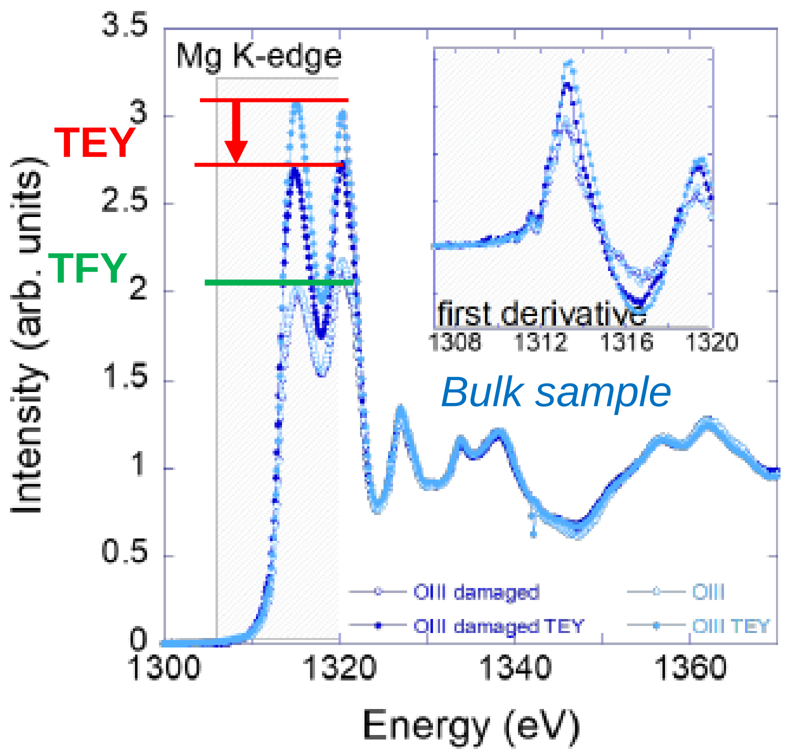

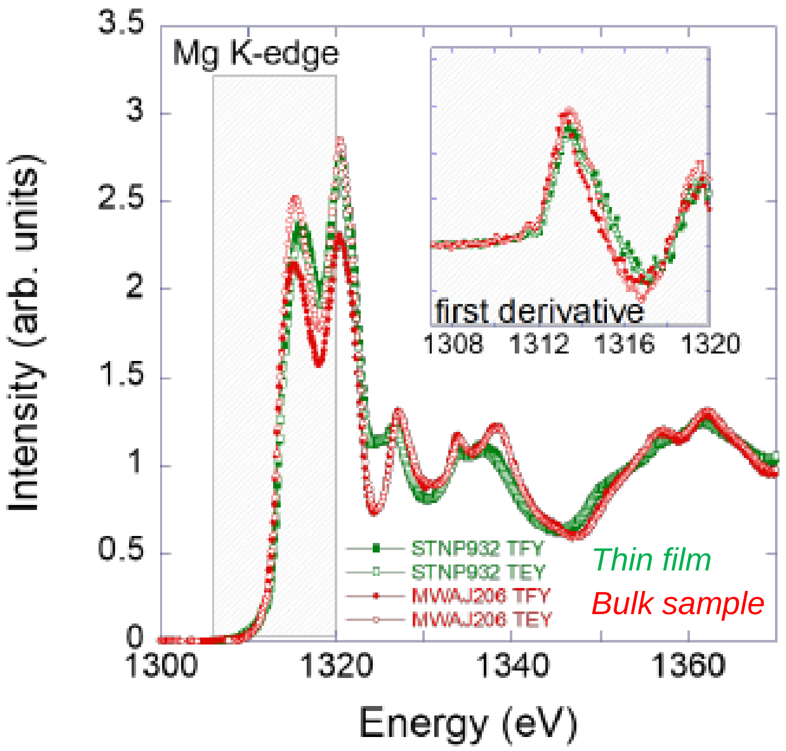

Bulk samples:

- Sharpening of pre-peaks for TEY as compared to TFY (self-absorption in TFY?)
- No damage pattern in TFY pre-peaks
- Damage pattern in TEY pre-peaks

- SNTP932 very similar in TFY and TEY.

→For 35 nm thickness: absence of self-absorption effects.

- Sharpening of pre-peaks for TEY versus TFY in MWAJ206 (self-absorption?)

Fourier Transforms Mg K-edge- MgF_2 bulk versus thin film

Drift in Mg-F first shell:
Thin film
→ Bulk crystal

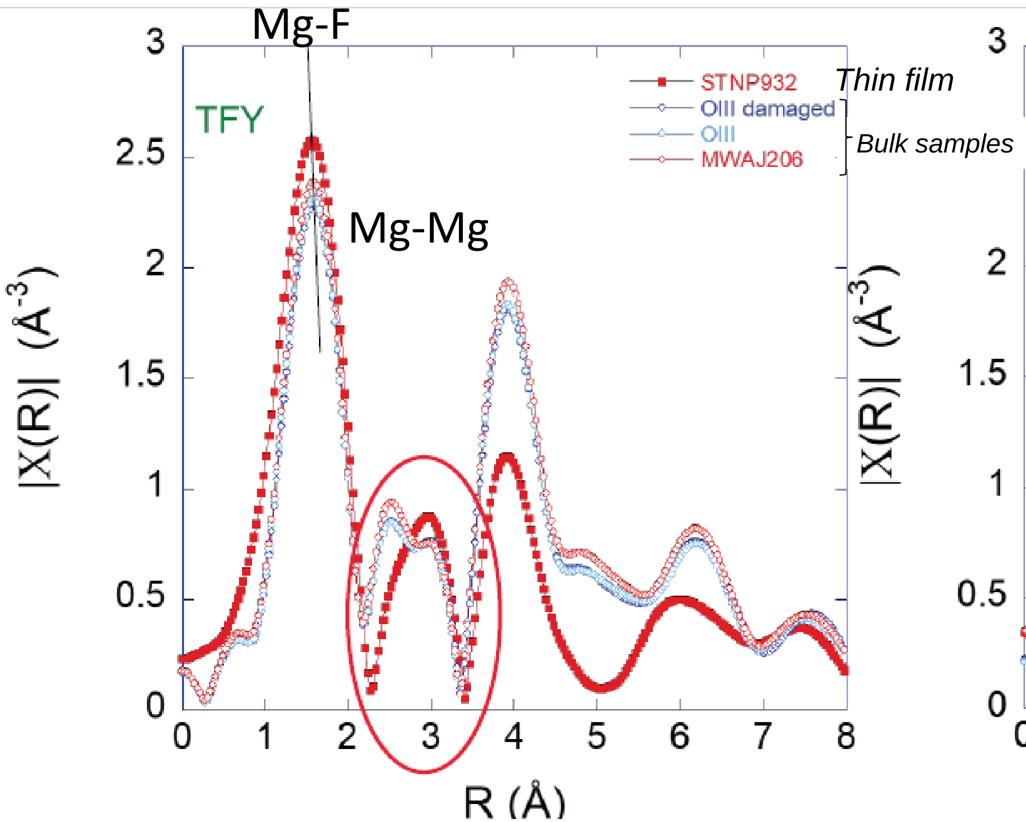

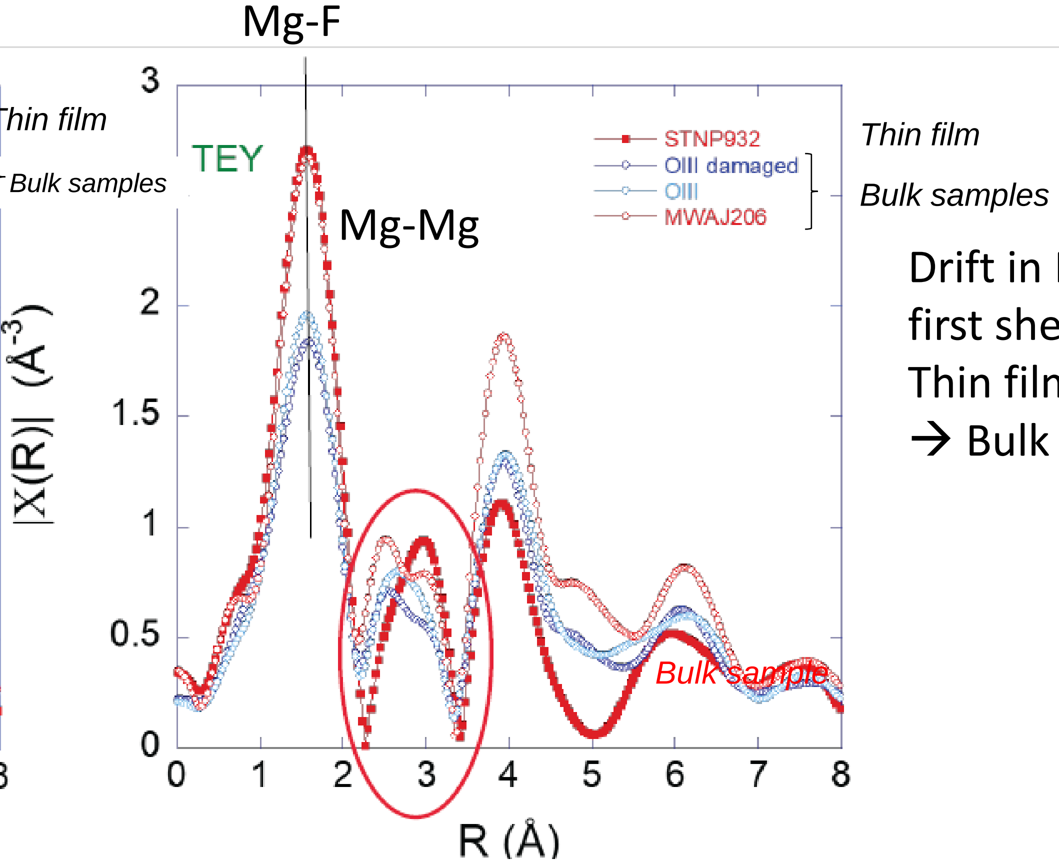

Drift in Mg-F first shell:
Thin film
→ Bulk crystal

- Single crystal structure better as thin film structure (as usual).
- 2nd shell for Mg-Mg strongly altered between bulk and thin film.
- OIII bulk data damaged/non-damaged very similar (as in XAS data).

- Single crystal structure better as thin film structure (as usual).
- Damage-induced structural changes in OIII TEY data (2nd shell)
- Why are MWAJ206 and OIII undamaged data not comparable?

EXAFS fits Mg K-edge – Summary

		R_{Mg-F} (Å)	ΔR_{Mg-F} (Å)	σ^2_{Mg-F} (Å^2)	$\Delta\sigma^2_{Mg-F}$ (Å^2)	R_{Mg-Mg} (Å)	ΔR_{Mg-Mg} (Å)	σ^2_{Mg-Mg} (Å^2)	$\Delta\sigma^2_{Mg-Mg}$ (Å^2)
Thin film	STNP932	2.006	0.010	0.0108	0.0019	3.001	0.050	0.0055	0.0087
Bulk sample	MWAJ206	2.004	0.020	0.0125	0.0039	2.864	0.094	0.008	0.017

"The fit of the first shell only and of the first two provided consistent results. The two-shell model included 6 F atoms expected at 1.9892 Å and 2 Mg atoms expected at 3.05 Å from the absorber (Mg). The table reports the best fit values (not phase shift corrected)."

"Most likely the Mg-Mg distance for the MgF2 p-Al thin film expand respect to the bulk material. This seems consistent with the Mg K-edge energy positions (Figure 1, inset)."

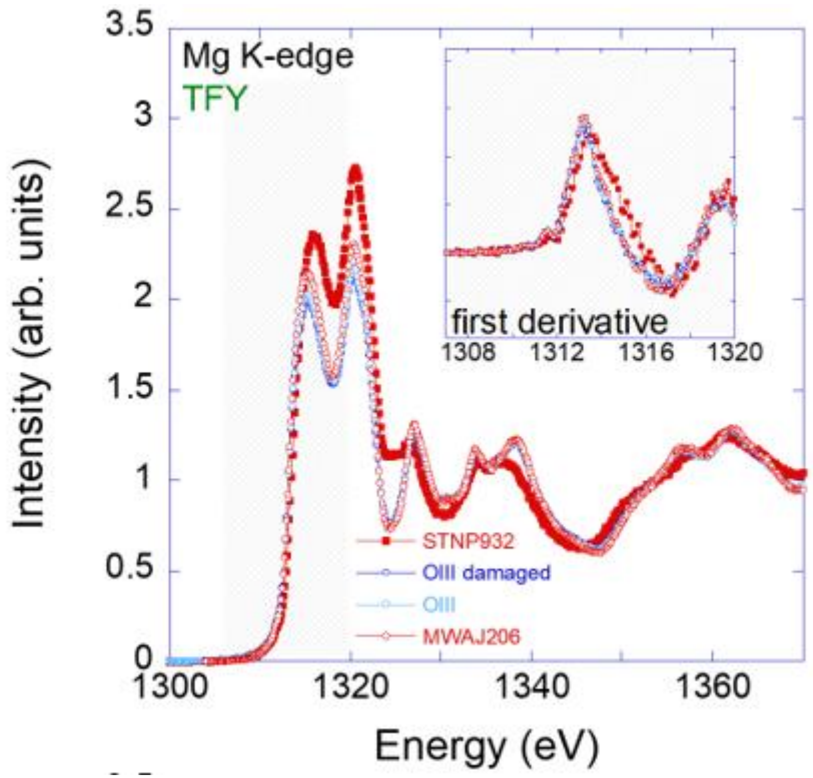

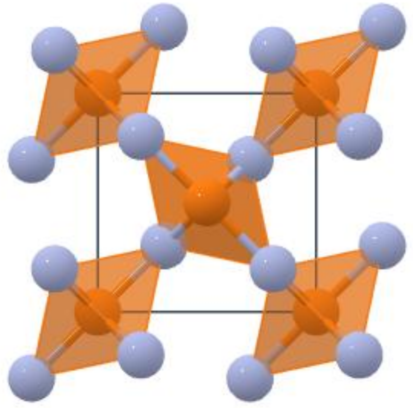

There are two shorter (1.98 Å) and four longer (1.99 Å) Mg–F bond lengths.

Ag 3d XPS Line

- Time sequence during **downstream** air plasma